Journal of Zhejiang University SCIENCE
ISSN 1009-3095
http://www.zju.edu.cn/jzus
E-mail: jzus@zju.edu.cn

Seismic force modification factor for ductile structures

TONG Gen-shu (童根树)[1], HUANG Jin-qiao (黄金桥)[1,2]

([1]*Department of Structural Engineering, Zhejiang University, Hangzhou 310027, China*)

([2]*China United Engineering Corporation, Hangzhou 310027, China*)

E-mail: tonggs@ccea.zju.edu.cn; huangjq@chinacuc.com

Received July 14, 2004; revision accepted Oct. 25, 2004

Abstract: The earthquake forces used in design codes of buildings should be theoretically determinable. This work examines the seismic force modification factor R based on elastic-plastic time-history earthquake analysis of SDOF systems, wherein the hysteresis models are elastic-perfectly-plastic (EPP), elastic-linearly-hardening (ELH), shear-slipped and bilinear-elastic. The latter two models are analysed for separating the effect of the ductility and the energy-dissipating capacity. Three-hundred eighty-eight earthquake records from different site conditions are used in analysis. The ductility is taken to be 2, 3, 4, 5 and 6, with the damping ratio being 0.02, 0.035 and 0.05 respectively. The post-yield stiffness ratios 0.0, 0.1 and 0.2 are used in the analysis. The R spectra are standardized by the characteristic period of the earthquake records, which leads to a much smaller scatter in averaged numerical results. It was found that the most important factor determining R is the ductility. R increases more than linearly with ductility. The energy-dissipating capacity, damping and the post-yield stiffness are the less important factors. The energy dissipating capacity is important only for structures with short period and moderate period ($0.3\leq T/T_g<5.0$). For EPP and ELH models, R for 0.05 damping is 10% to 15% smaller than for 0.02 damping. For EPP and ELH models, greater post-yield stiffness leads to greater R, but the influence of post-yield stiffness is obvious only when the post-yield stiffness is less than 10% of the initial stiffness. By means of statistical regression analysis the relation of the seismic force modification factor R with the natural period of the system and ductility for EPP and ELH models were established for each site and soil condition.

Key words: Aseismic design, Seismic force modification coefficient, Ductility, Energy-dissipating capacity
doi:10.1631/jzus.2005.A0813 **Document code:** A **CLC number:** TU391

INTRODUCTION

In codes for seismic design of buildings of many developed countries, elastic response spectra are adopted to calculate the base shear forces. For example, the base shear defined in Japan code 1997 is:

$$F_{EK}=D_sF_{es}C_0ZA_iR_tW \quad (1)$$

where R_t is the elastic design spectrum; D_s is the structural coefficient changing among 0.25 to 0.50 to take account of different ductility of different structures; W is the total weight of a structure; the others are site coefficient, irregularity coefficient, etc. Another example is the base shear defined in the United States UBC1997:

$$V=C_VIW/RT \quad (2)$$

where I is the importance coefficient; T is the structural period of vibration; C_V represents soil type of site and zone. R is the system performance coefficient, introduced to reduce the elastic earthquake force considering the beneficial effects of ductility and energy-dissipating capacity of a structure. R varies from 4.5 for structures with poor ductility to 8.5 for structures with good ductility and good energy-dissipating capacity. EC8 (Europe code for seismic design of buildings) also introduces a coefficient q (equals 2 to 5) to modify the elastic base shear. The Greece code is similar to EC8, the Canadian code is close to the American code. These were reported by Xu and Yu (1998).

The base shear in the Chinese code (GB50011-2001) is given as:

$$F_{EK}=\alpha_1G_{eq} \quad (3)$$

where G_{eq} is the total effective weight of structures; α_1 is an earthquake coefficient determined by the elastic spectrum multiplied by a coefficient 0.35. This method neglects the difference in ductility and energy-dissipating capacity of different structures. This provision does not accord with the current aseismic philosophy that increasing energy-dissipating capacity and ductility will decrease the destructive effect of earthquake.

With the development of numerical technology, it is now possible to determine the seismic force modification coefficient R (abbreviated as SFMC hereafter) by theoretical analysis. Many studies were reported in literature, such as Newmark and Hall (1982), Krawinkler and Nassar (1992), Miranda and Bertero (1994), Vidic *et al*.(1994), Li *et al*.(1999), Kappos (1999), Miranda (1993), Borzi and Elnashai (2000), Zhuo and Fan (2001). From the available study results, we can see that earthquake magnitude and epicenter distance have no great influence on R, but ductility, period of structures, shape of hysteresis loop and site profile have. These studies considered only short-period structure (<3 s), 5% damping and 3 soil types, the hysteresis model is either Clough's or bilinear. Their results were not been normalized by the characteristic periods of earthquake records, so their results have relatively great statistical variance. In China, there are 4 soil profile types, for steel structures the damping is 2% and the shape of the hysteresis curve is bilinear with possible post-yield stiffness. Additional information is needed for these cases.

This work examines the R-coefficient based on elastic-plastic earthquake time-history analysis of SDOF systems; the hysteretic models are EPP (elastic-perfectly-plastic), ELH (elastic-linearly-hardening), shear-slipped and bilinear elastic (i.e. elastic-plastic without energy-dissipating capacity) (Fig.1). The three-hundred eighty-eight earthquake records were used in the analysis taken from 4 site with different soil conditions. Ductility of 2, 3, 4, 5 and 6 were assigned to the systems in the analysis. Totally more than 480000 pieces of data were obtained from which R was evaluated by statistical regression analysis. For the EPP and ELH models, the variation of R with the system natural period and ductility was established for each site and soil condition, and the effects of damping and the post-yield stiffness on R were also obtained. The R spectra were standardized by the characteristic period of the earthquake records, which leads to much smaller scatter in the numerical results.

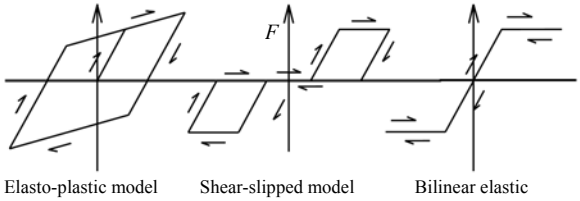

Fig.1 Hysteresis loop models

EARTHQUAKE RECORDS FOR ANALYSIS

The main earthquake records used in the following analysis are shown in Table 1, they were downloaded from the website (http://peer.berkeley.edu). All these records were horizontal components of corresponding earthquakes. All records were scaled to have a maximum acceleration of $0.2g$ to provide a common basis for comparison. Among 388 records, 112 records were taken from Site type I, 88 records from Site type II, 114 from Site type III and 74 from Site type IV, according to the Chinese Code (2001), but there were 3 Site types according with many countries Code. So, many records belong to different Site types of China and other countries.

These records have different epicentres. The current available results obtained by Miranda and Bertero (1994) and Vidic *et al*.(1994) showed that the earthquake magnitude and the epicentre have negligible effects on the SMFC, so these factors are not considered in this paper.

APPROADCH TO DETERMINE SFMC THEORETICALLY

The dynamic equilibrium equation of a SDOF system is:

$$m\ddot{y} + c\dot{y} + ky = -m\ddot{a} \tag{4}$$

where m is the mass; y is the displacement; c is the damping; k is the tangent stiffness; $\ddot{a}$ is the earthquake acceleration record.

Table 1 The main earthquake records used in calculation

Earthquake	Time
Anza (USA)	1980-2-25 10:47
Cape Mendocino (USA)	1992-4-25 18:06
Landers (USA)	1992-6-28 11:58
Loma Prieta (USA)	1989-10-18 00:05
Northridge (USA)	1994-1-17 12:31
San Francisco (USA)	1957-3-22 19:44
Borrego Mtn (USA)	1968-4-9 02:30
Livermore (USA)	1980-1-24 19:00
Lytle Creek (USA)	1970-9-12 4:30
Borrego (USA)	1942-10-21 16:22
Coalinga (USA)	1983-5-2 23:42
Imperial Valley (USA)	1979-10-15 23:16
Imperial Valley (USA)	1979-10-16 06:58
Chi-Chi (PRC TAIWAN)	1999-09-20
Kobe (JAPAN)	1995-1-16 20:46
Gazli (USSR)	1976-05-17
Georgia (USSR)	1991-06-15
New Zealand	1987-03-02
Coyote Lake (USA)	1979-8-6 17:05
Hollister (USA)	1974-11-28 23:01
N. Palm Springs (USA)	1986-7-8 09:20
San Fernando (USA)	1971-2-9 14:00
Whittier Narrows (USA)	1987-10-1 14:42
Kern County (USA)	1952-7-21 11:53
Livermore (USA)	1980-1-27 02:33
Morgan Hill (USA)	1984-4-24 21:15
Central Calif. (USA)	1954-4-25 20:33
Central Calif. (USA)	1960-1-20 03:26
Imperial Valley (USA)	1979-10-15 23:19
Kocaeli (Turkey)	1999-8-17
Duzce (Turkey)	1999-11-12
Superstitn Hills (U. K.)	1987-11-24 13:16
Westmorland (U. K.)	1981-4-26 12:09
Friuli (Italy)	1976-09-15
Nahanni (Canada)	1985-12-23
Victoria (MEXICO)	1980-6-9 03:28
Total	388 (records)

As widely known, every real structure has a limited ductility. In a nonlinear system subjected to a specific earthquake, if the yield force is very small, it will have large elastic-plastic displacement exceeding the available ductility. In order to restrict the displacement response within the available ductility, the yield force must be increased. Denoting the required minimum yield force of a system with available ductility μ by $F_{y\mu}$, the maximum force response of a linear elastic system by F_e, the SFMC R may be defined by:

$$R=F_e/F_{y\mu} \tag{5}$$

The flowchart for calculating R is shown in Fig.2, standardization process was appended comparing with the procedure of other researches; where k_0 is the initial stiffness of the system; ξ is the damping ratio; α is the ratio of post-yield stiffness to the initial stiffness; $F(t)$ is the earthquake input. Repeating this process for a given earthquake record and a given system ductility while varying the system period, we obtain a normalized SFMC spectrum. While other researchers did not add a standardization process in the procedure by using the characteristic period T_g of the earthquake record to obtain an SFMC spectrum, this standardization eliminates partly the effect of different earthquake records on the SFMC spectrum.

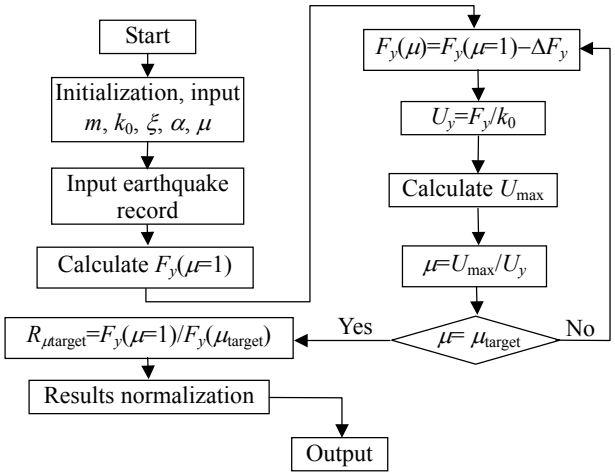

Fig.2 Flowchart for SFMC calculation

The standardized SFMC spectra for a given ductility and a given set of parameters obtained by calculating all earthquake records of the same Site types were put together to carry out statistical regression analysis. The average spectra found are given in the following sections for each set of parameters. Covariance spectrum is also given for each set of parameters.

Central acceleration method was used in the elastic-plastic dynamic analysis to avoid numerical damping. For each earthquake record, the system period of the SDOF is increased from 0.1 s to 6.0 s with increment of 0.1 s. For records with very long characteristic period T_g, for example in records from Taiwan, the system period of the SDOF is increased from 0.1 s to $5T_g$. Consequently the number of samples may be smaller for Site type IV when the SFMC

involves non-dimensionalized coordinates T/T_g and T/T_g>5. But there are 30 records of each Site type at least near to 6.0 s. It is enough for the spectra to be meaningful. The ductility is changed from μ=1 (elastic) to 6.0 with increment 1.0. The damping ratio ξ is taken to be equal to 0.02, 0.035 and 0.05 respectively; the post-yield stiffness coefficient α is taken as 0.0 (EPP), 0.1 and 0.2 respectively.

Three hysteresis models are shown in Fig.1. Most of this paper is on the EPP and ELH model. The shear-slipped model represents a limited and one-off energy-dissipating capacity. The bilinear elastic model represents a structure with ductility but without any energy-dissipating capacity. These two models were analyzed to separate the effects of ductility and the energy-dissipating capacity. In the currently available literature, these two factors are always mixed together.

SFMC *R* FOR EPP AND ELH MODELS

Currently available analyses results showed that the most important factor determining *R* is the ductility. The Site type also has great influence. Li *et al*.(1999) studied the EPP and ELH hysteresis models and found that *R* increases with post-yield stiffness, but that the effect of which is limited. *R* increases faster when the ratio α of post-yield stiffness to elastic stiffness is less than 0.1 than when α is greater than 0.1. When α=0.15, *R* is 16%~27% greater than that of the EPP system.

The SFMC for a given hysteresis model may be expressed as a function of the ductility, damping ratio and the post-yield stiffness. In this paper it is expressed as the product of three parameters for each Site type:

$$R=R_\mu R_\xi R_\alpha \tag{6}$$

where R_μ is the SFMC for EPP model under a damping of 0.05; R_ξ is a coefficient considering the effect of reduced damping; R_α is a coefficient considering the effect of post-yield stiffness.

DUCTILITY COEFFCIENT R_μ

The averaged SMFC R_μ for EPP model under a damping of 0.05 for the four Site types are given in Fig.3 showing that for a given ductility, the standardized SFMC spectra at Site types I, II, III and IV differ little. All the curves converge to μ when the system period increases further. When T/T_g<1, the SFMC increases almost linearly from 1.0 for a rigid system to approximately μ at T/T_g=1, the enlarged figures are shown in Fig.4 for the short period range. When T/T_g>1, the SFMC varies very little with the system period, and may be approximated safely by a horizontal line, i.e. (Vidic *et al*., 1994; Fajfar, 1995):

$$R_\mu=\begin{cases}1+(\mu-1)T/T_g, & 0\le T\le T_g\\ \mu, & T\ge T_g\end{cases} \tag{7}$$

Here no difference is made among Site types I, II, III and IV for simplicity and safety.

DAMPING COEFFICIENT R_ξ

Dividing the SFMC for ξ=0.02 and 0.035 by the SFMC for ξ=0.05, we obtain the damping coefficient R_ξ. Fig.5 shows this coefficient under different ductility. It is seen from Fig.5 that these coefficients are very close under different ductility, because of this phenomenon, R_ξ spectra are established by summing these coefficients and averaging them. The averaged damping coefficients R_ξ for four Site types and different post-yield stiffness are given in Figs.6a~6d, showing that the site conditions and post-yield stiffness also have very limited influence on R_ξ. The R_ξ spectra in Figs.6a~6d show that R_ξ is greater when the damping ratio is small, and that the damping is more efficient in reducing the seismic response of a stiffer system. When the system period increases, the influence of the damping decreases. When the system period increases to a certain value (*T*=6 s taken in this paper for the sake of safety), R_ξ approaches 1.0.

The damping is useful for aseismic design because it dissipates energy during earthquake, and at the same time the system also has the capacity of dissipating energy through plastic deformation. By weakening the development of plastic deformation through reducing the displacement response, the damping reduces the SFMC. The SFMC when the damping is 0.05 is 10%~18% smaller than the SFMC when the damping ratio is 0.02.

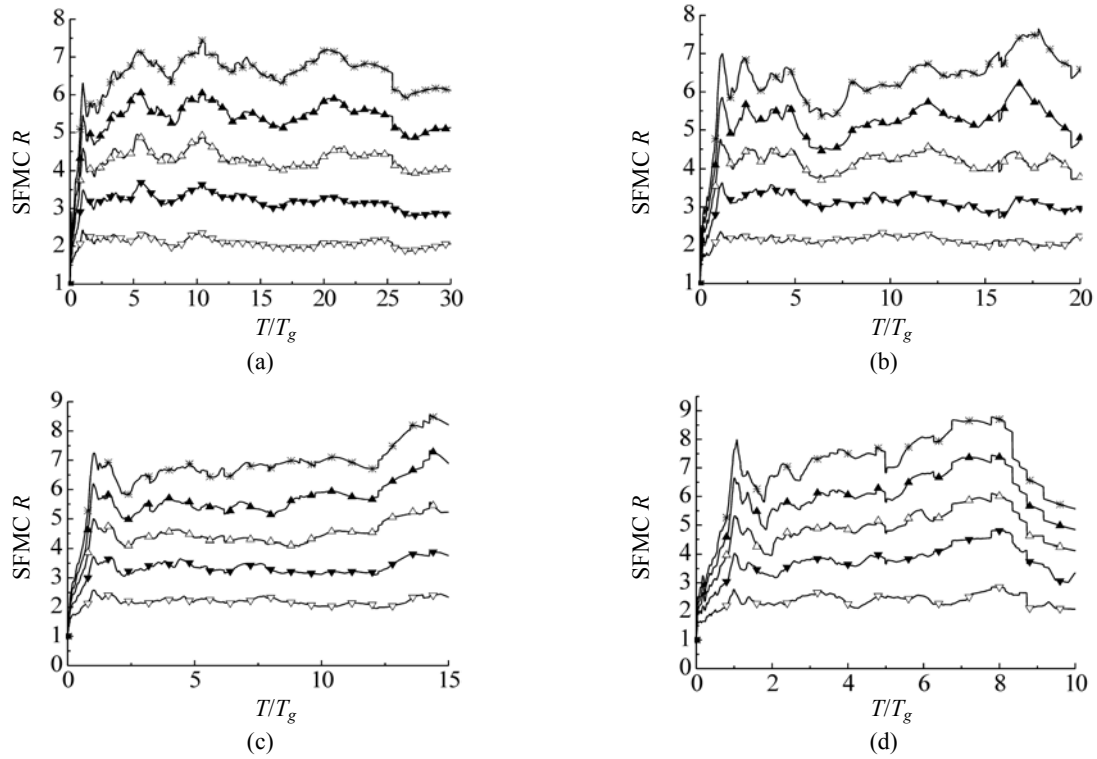

Fig.3 Ductility coefficient (α=0.0, ξ=0.05). (a) Site type I; (b) Site type II; (c) Site type III; (d) Site type IV

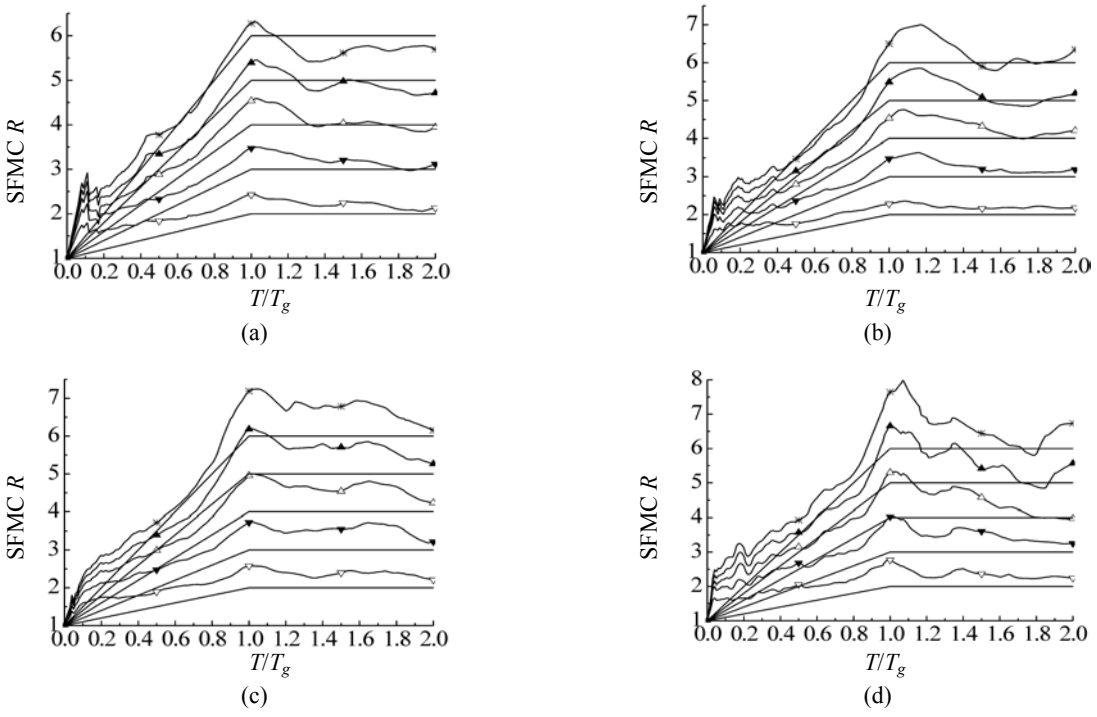

Fig.4 Enlarged figures of ductility coefficient in short period range (α=0.0, ξ=0.05)
(a) Site type I; (b) Site type II; (c) Site type III; (d) Site type IV

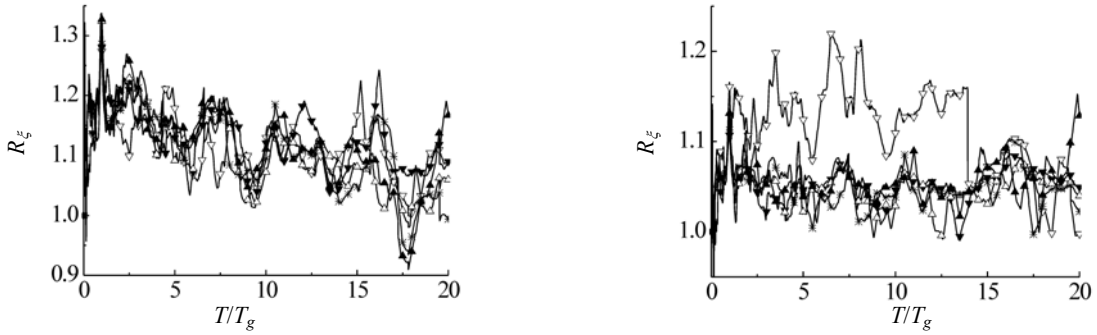

Fig.5 Damping coefficient of Site type II without post-yield stiffness (α=0.0). (a) Damping ratio 0.02/damping ratio 0.05; (b) Damping ratio 0.035/damping ratio 0.05 μ=2 μ=3 μ=4 μ=5 μ=6

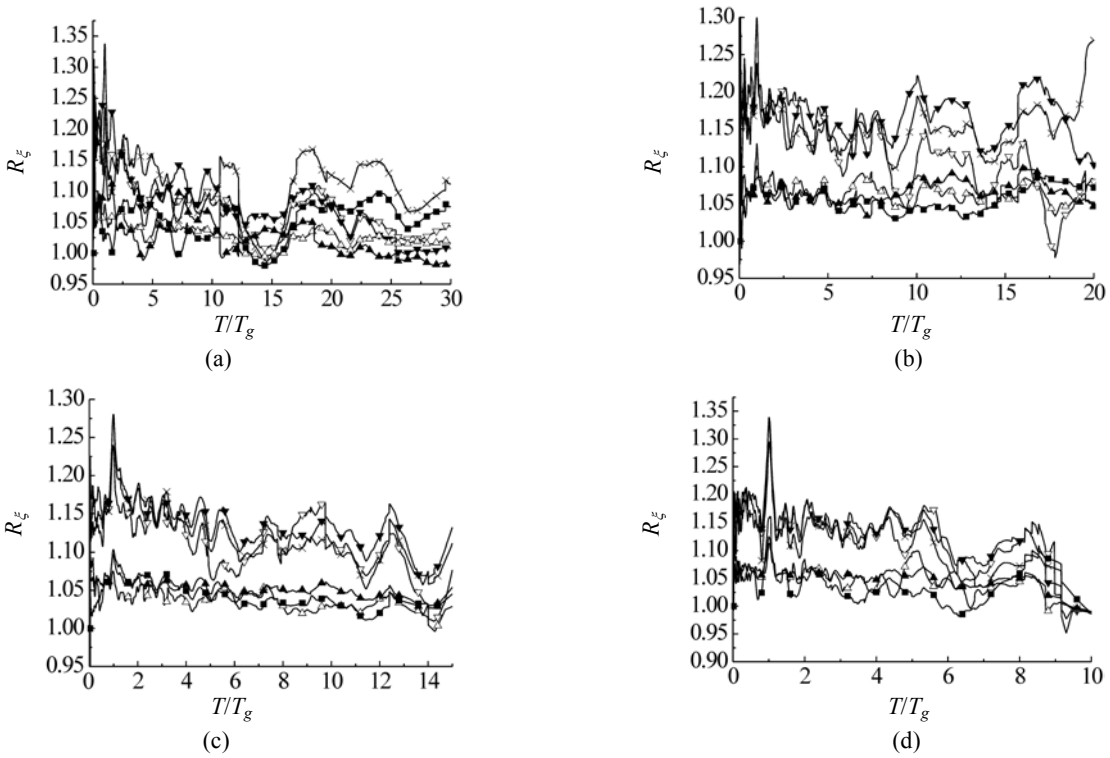

Fig.6 Damping coefficient $R_{\xi 0.02(0.035)}/R_{0.05}$ (α=0.0). (a) Site type I; (b) Site type II; (c) Site type III; (d) Site type IV

$\alpha(0.0)\xi(0.02)$ $\alpha(0.1)\xi(0.02)$ $\alpha(0.2)\xi(0.02)$ $\alpha(0.0)\xi(0.035)$ $\alpha(0.1)\xi(0.035)$ $\alpha(0.2)\xi(0.035)$

In this way, the seismic force seems to be greater when the damping is 0.05 than when damping is 0.02. Actually, because the elastic force F_e is about 32% smaller when the damping is 0.05 than when the damping is 0.02 (Chinese code, 2001), the final seismic force decreased, and considering the beneficial effects of both the damping and the plasticity, becomes still smaller when the damping is 0.05 than when the damping is 0.02 damping ratio, but not to the same extent as in the case of elastic systems.

The damping coefficient R_ξ may be approximated by:

$$R_\xi = 1 + (0.49 - 2.19\sqrt{\xi})(1 - T/6) \tag{8}$$

POST-YIELD STIFFNESS COEFFICIENT R_α

Dividing the SFMC for α=0.1 and 0.2 by the

SFMC for α=0.0, we obtain the post-yield stiffness coefficient R_α. Fig.7 shows this coefficient under different ductility. It is seen from Fig.7 that this coefficient increases with ductility, but when $\mu \geq 5$, they are nearly the same. It may also be seen that R_α are nearly the same for α=0.1 and α=0.2. But when $0 \leq \alpha \leq 0.1$, it increases with the post-yield stiffness (Li *et al*., 1999).

In Figs.8a~8d, these coefficients under different ductility are summed together and averaged to examine the effect of different damping and different post-yield stiffness for four Site types. It is seen that this averaged coefficient R_α is nearly independent of the damping ratio and the post-yield stiffness.

From Figs.8a~8d, it may be seen that for different Site types R_α varies differently with the system

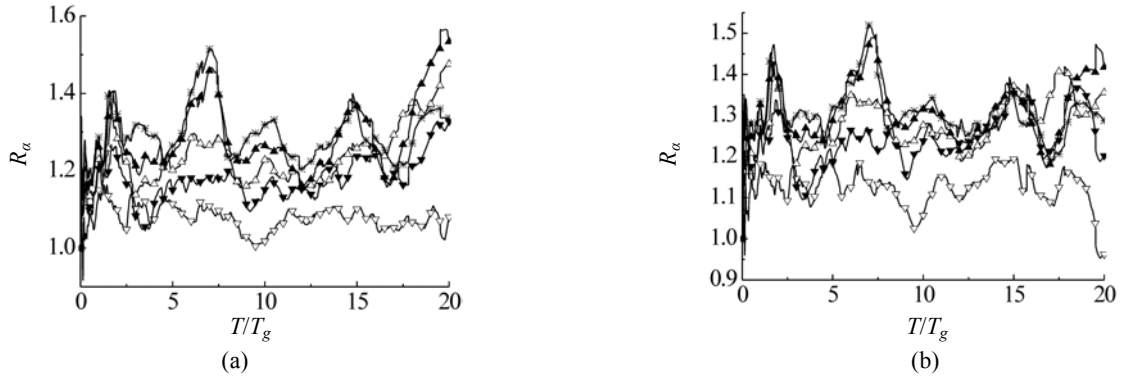

Fig.7 Post-yield coefficient of Site type II damping ratio 0.05. (a) Post-yield stiffness 0.1/post-yield stiffness 0.0; (b) Post-yield stiffness 0.2/post-yield stiffness 0.0 μ=2 μ=3 μ=4 μ=5 μ=6

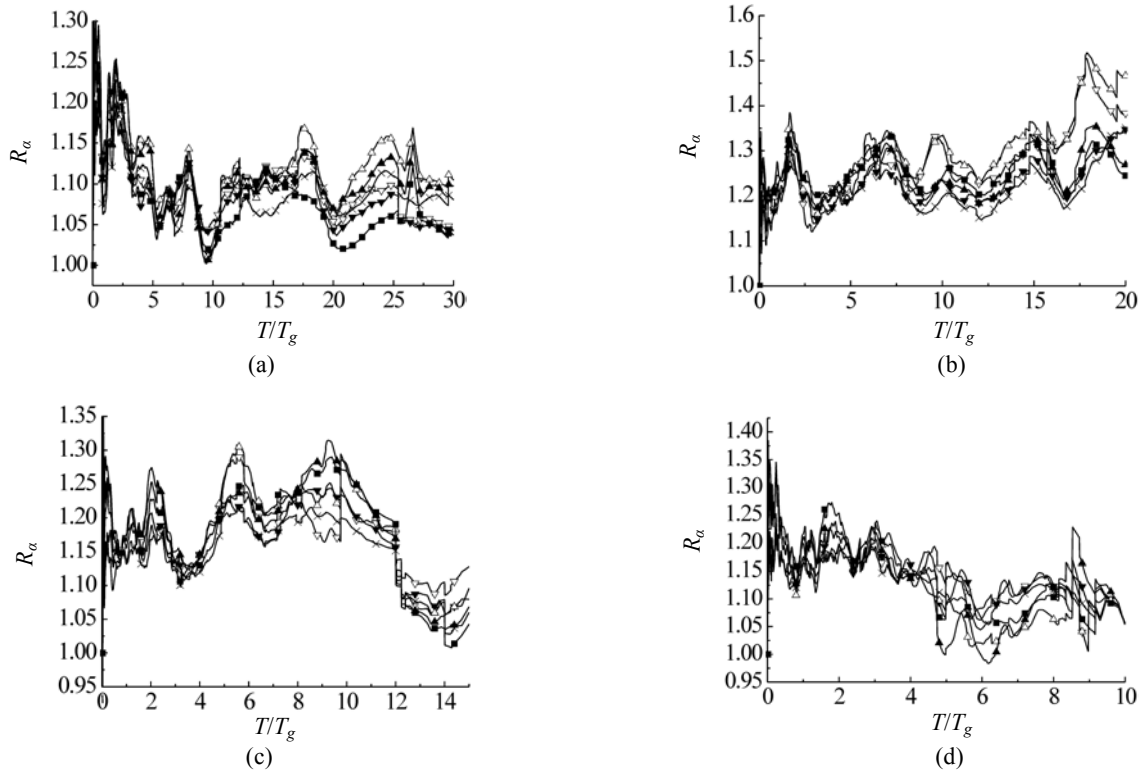

Fig.8 Post-yield stiffness coefficient. (a) Site type I; (b) Site type II; (c) Site type III; (d) Site type IV

$\alpha(0.1)\xi(0.02)$ $\alpha(0.1)\xi(0.035)$ $\alpha(0.1)\xi(0.005)$ $\alpha(0.2)\xi(0.02)$ $\alpha(0.2)\xi(0.035)$ $\alpha(0.2)\xi(0.05)$

period.

Theoretically, when the system period is very large R_α will approach 1.0. When α=0.0, R_α=$R_{0.0}$=1.0. Based on Fig.7 and Fig.8, we formulate the following expression for $R_{0.1}$:

For Site type I:

$$R_{0.1}=\begin{cases}(1.15-T/90T_{\mathrm{g}})\gamma, & 0\le T\le 9T_{\mathrm{g}}\\ 1.05\gamma, & 9T_{\mathrm{g}}\le T\le 6\mathrm{s}\end{cases} \tag{9a}$$

For Site type II:

$$R_{0.1}=1.15\gamma,\quad 0\le T\le 6\mathrm{s}; \tag{9b}$$

For Site type III:

$$R_{0.1}=1.15\gamma,\ 0\le T\le 6\mathrm{s}; \tag{9c}$$

For Site type IV:

$$R_{0.1}=(1.15-T/60)\gamma,\ 0\le T\le 6\mathrm{s}; \tag{9d}$$

where $\gamma=\dfrac{1+0.125\sqrt{\mu-1}}{1.15}$. (10)

R_α is formulated as follows:

$$R_\alpha=\begin{cases}1+10\alpha(R_{0.1}-1) & 0\le\alpha\le 0.1\\ R_{0.1} & \alpha>0.1\end{cases} \tag{11}$$

COVARIANCE OF *R*

Figs.9a~9d show the covariance of the SFMC for EPP model and 0.02 damping of four Site types. It can be seen that the covariance does not change with the ductility. For different damping and post-yield stiffness, the covariance is similar. They are omitted here for brevity. But it may be mentioned that when the damping is increased, the covariance is slightly decreased. When the post-yield stiffness is increased, the covariance is also decreased slightly.

The covariance for four Site types may be approximated by

$$C_{\mathrm{var}}=0.3 \tag{12}$$

COMPARISON OF PROPOSED FORMULA FOR *R* AND ITS PRACTICAL APPLICATION

The SFMC *R* should satisfy the following conditions: (1) when *T*=0, *R*(*T*=0)=1, this is because a rigid system will move with site synchronously dur-

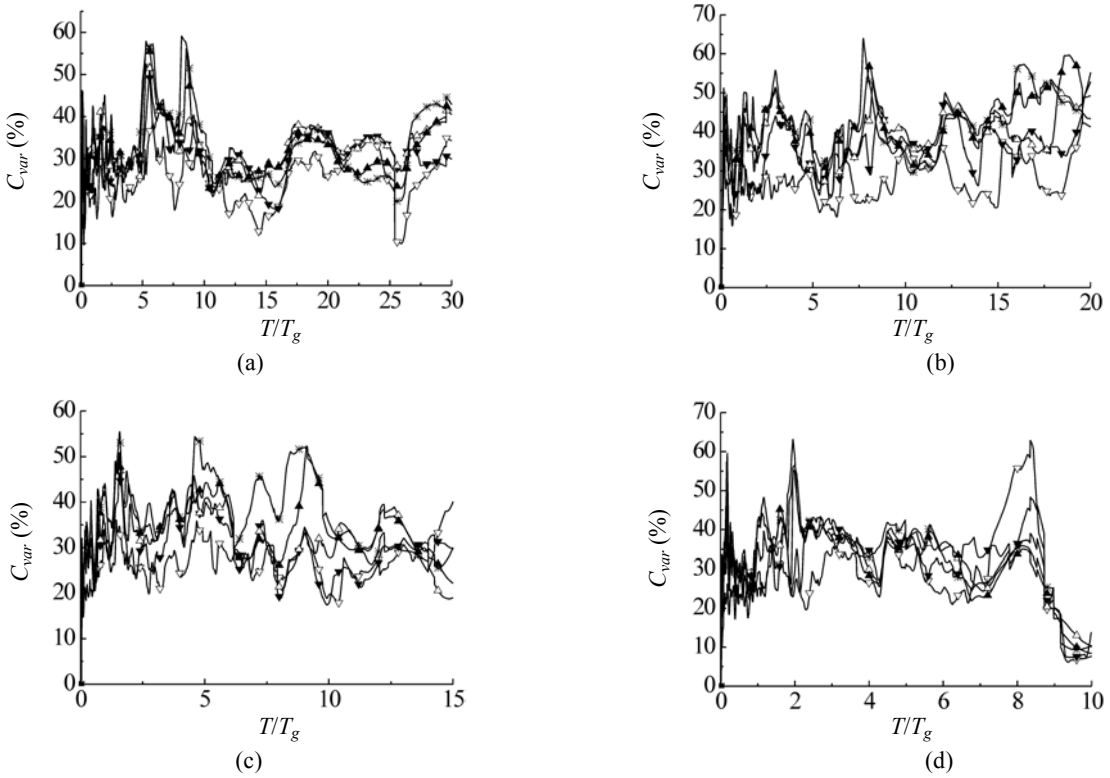

Fig.9 Covariance of SFMC. (a) Site type I; (b) Site type II; (c) Site type III; (d) Site type IV

ing earthquakes; (2) when $T\to\infty$, $R(T\to\infty)\to\mu$, i.e. the relative displacement of an infinite flexible system is equal to movement of the site during earthquake, regardless of the elastic-plastic behavior; (3) when the system is elastic, μ=1, $R(T, 1)$=1. The final SFMC is given by Eq.(6).

Comparisons of Eqs.(6) to (11) with the numerical analysis, are shown in Fig.10.

Fig.10 shows that the proposed formula approximates the numerical results reasonably well. In general, the proposed equation is on the safe side. The spectra of R for other site profile types were presented in Huang (2005).

The proposed equation has greater deviation with numerical results for Site type IV, because many earthquake records for Site type IV come from Taiwan, where they have very large site characteristic period and complicated frequency compositions, although the analysis shows a greater SFMC for this Site type, a lower R is proposed for the sake of safety.

If the proposed SFMC R is used in practice, reliability must be considered. Denoting the SFMC used in practice by R_D, then

$$R_D = R[1-\beta C_{var}] \tag{13}$$

β is taken to be 1.0, 1.645 or 2.0, depending on the reliability required by different codes.

SFMC FOR SHEAR-SLIPPED AND BILINEAR ELASTIC MODELS

In this section we investigate the SFMC when the hysteresis model is either shear-slipped or bilinear elastic. These models are used to separate the effect of ductility and the energy dissipating capacity. The shear-slipped model has a one-off energy-dissipating capacity, while the bilinear elastic model has no energy-dissipating capacity at all. Only Site type II is considered.

Figs.11a, 11b, 11c compare the SFMC spectra of three hysteresis models in the short period range (T/T_g<2.0), Figs.11d, 11e, 11f compare SFMC spectra in the long period range. From these figures, we see that in the short period range (T/T_g<1.0), the larger the energy dissipating capacity is, the greater the SFMC. The order of R from higher to lower value for different models in short period range of the systems is elasto-plastic>shear-slipped>bilinear elastic. In the middle period range (1.0≤T/T_g<5.0) the effect of en-

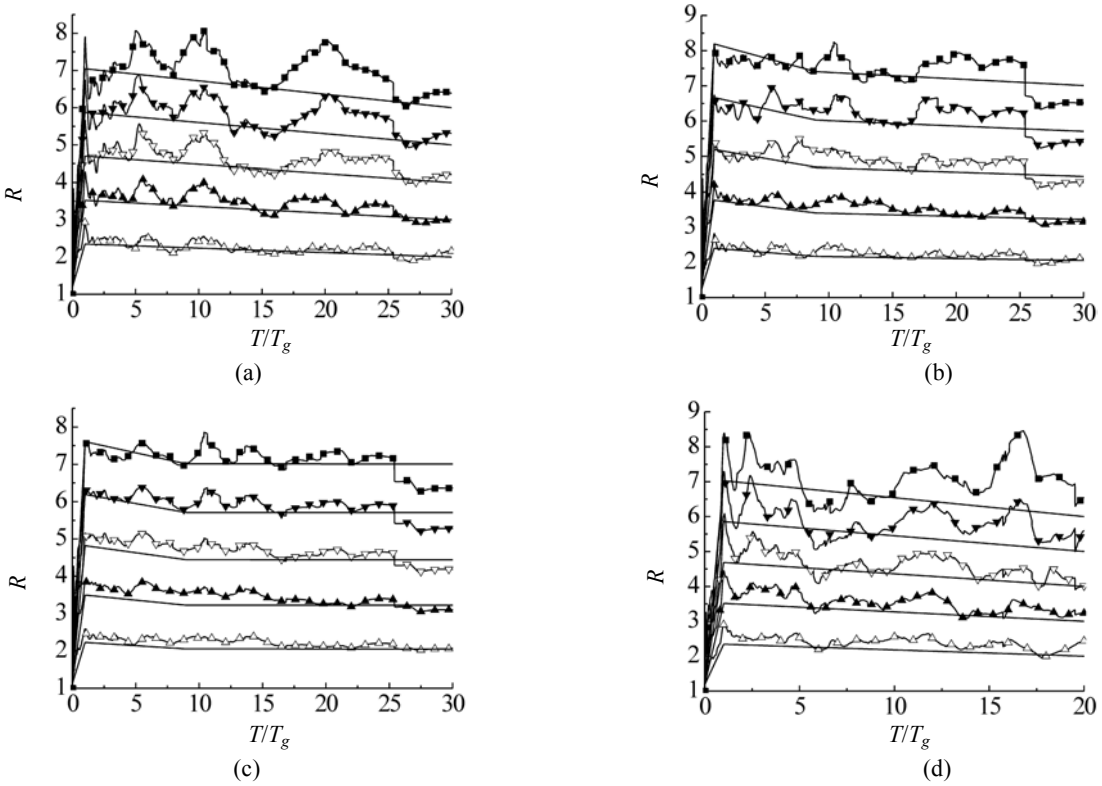

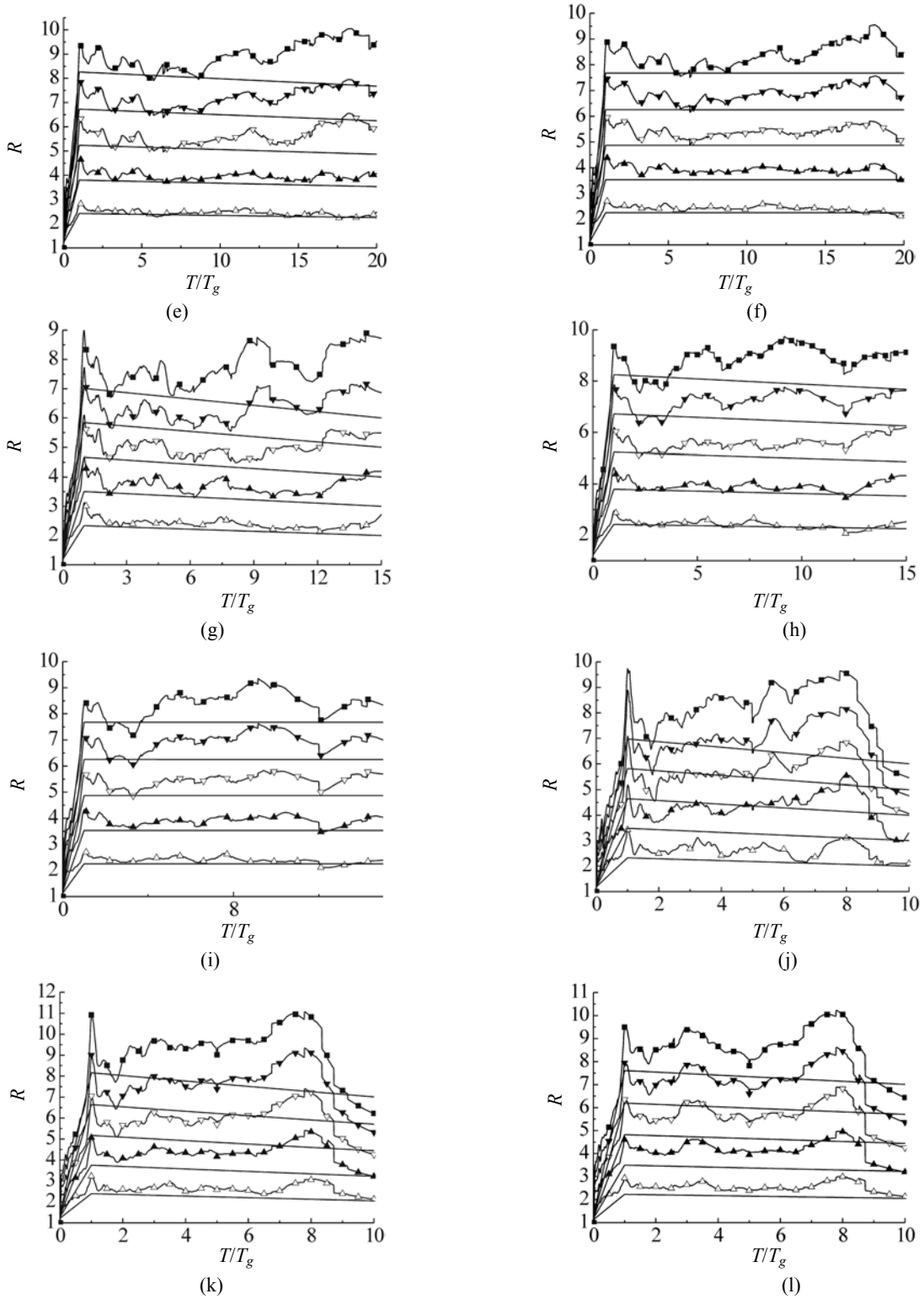

Fig.10 Comparison of Eqs.(6) to (11) with averaged SFMC spectra

(a) R of Site type I with α=0.0 and ξ 0.02; (b) R of Site type I with α=0.1 and ξ 0.035; (c) R of Site type I with α=0.2 and ξ 0.05; (d) R of Site type II with α=0.0 and ξ 0.02; (e) R of Site type II with α=0.1 and ξ 0.035; (f) R of Site type II with α=0.2 and ξ 0.05; (g) R of Site type III with α=0.0 and ξ 0.02; (h) R of Site type III with α=0.1 and ξ 0.035; (i) R of Site type III with α=0.2and ξ 0.05; (j) R of Site type IV with α=0.0 and ξ 0.02; (k) R of Site type IV with α=0.1 and ξ 0.035; (l) R of Site type IV with α=0.2 and ξ 0.05

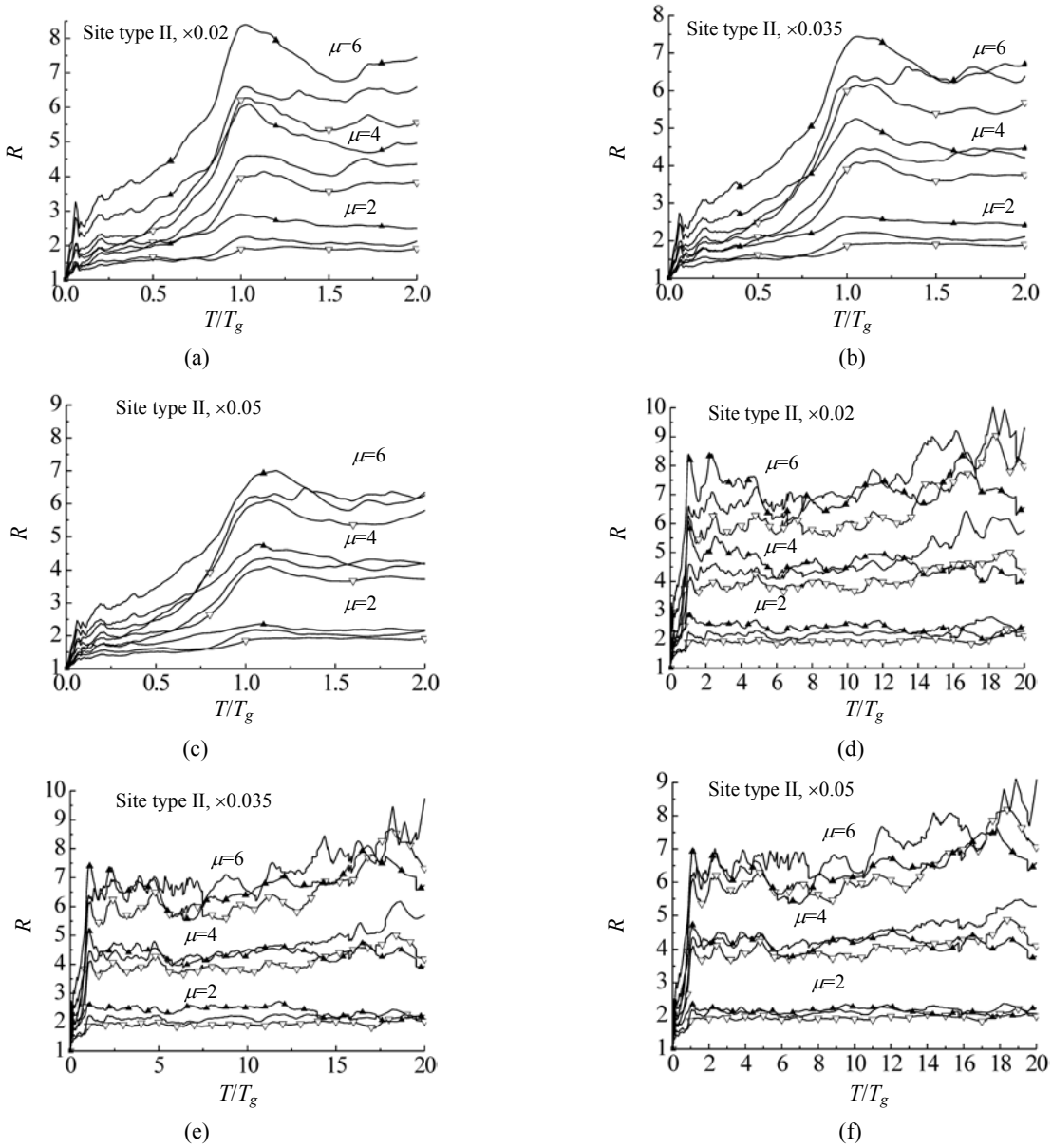

Fig.11 Influence of hysteresis models. (a) Damping ratio 0.02; (b) Damping ratio 0.035; (c) Damping ratio 0.05; (d) Damping ratio 0.02; (e) Damping ratio 0.035; (f) Damping ratio 0.05 —▽— Bilinear elastic; —▲— Shear-slipped; —△— EPP

ergy dissipating capacity is reduced, but the order is not changed. In the long period range ($T/T_g \geq 5.0$), the effect of energy dissipating capacity is not so obvious, but it can still be observed that the SFMC for bilinear elastic model is the smallest, and close to the ductility μ mostly.

Figs.12a~12c and Figs.13a~13c show the covariance of the SFMC for bilinear elastic and shear-slipped models under Site type II. It can be seen that the covariance for SS and BIL models is greater than that for the EPP model when the ductility is large.

From these figures we can also see that the damping ratio has no visible difference in its effects on the SFMC spectra for the shear-slipped model and the bilinear elastic model.

CONCLUSION

The earthquake forces used in design codes of buildings should be theoretically determinable. This

work studied the seismic force modification factor R based on elastic-plastic time-history earthquake analysis of SDOF system. The hysteresis models are ideal EPP, elastic-linearly-hardening, shear-slipped and bilinear-elastic, the latter two models were analyzed to separate the effect of the ductility and the energy-dissipating capacity. Three-hundred eighty-eight earthquake records were used in analysis. The ductility is taken to be 2, 3, 4, 5 and 6, and the damping ratio is 0.02, 0.035 and 0.05 respectively.

The post-yield stiffness ratios 0.0, 0.1 and 0.2 were used in the analysis. Normalization was carried out for SFMC spectra using the characteristic period T_g of the earthquake record. This standardization eliminates partly the effect of different earthquake records on the SFMC spectrum.

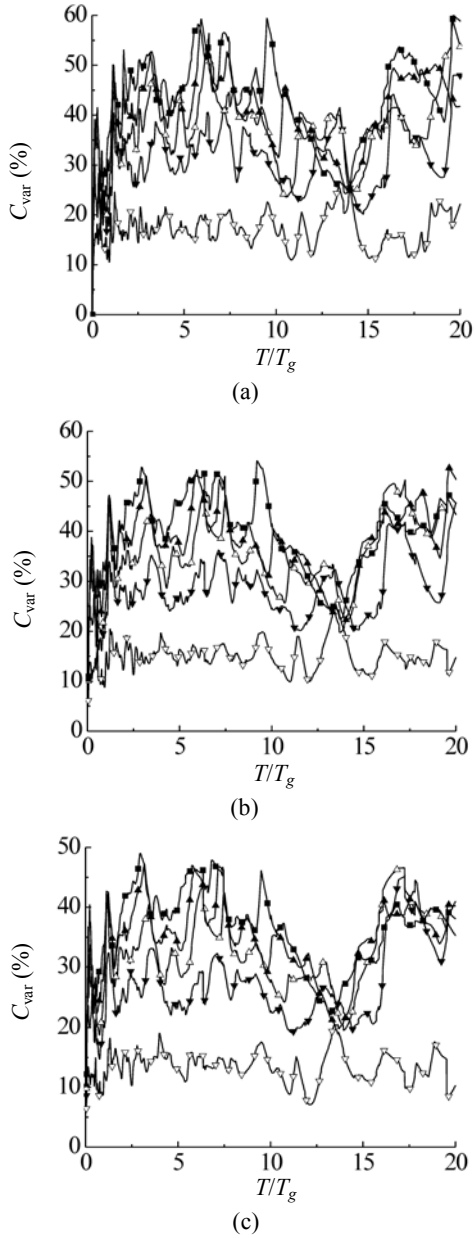

Fig.12 Covariance of SFMC in Site type II for bilinear elastic. (a) Damping ratio 0.02; (b) Damping ratio 0.0235; (c) Damping ratio 0.05

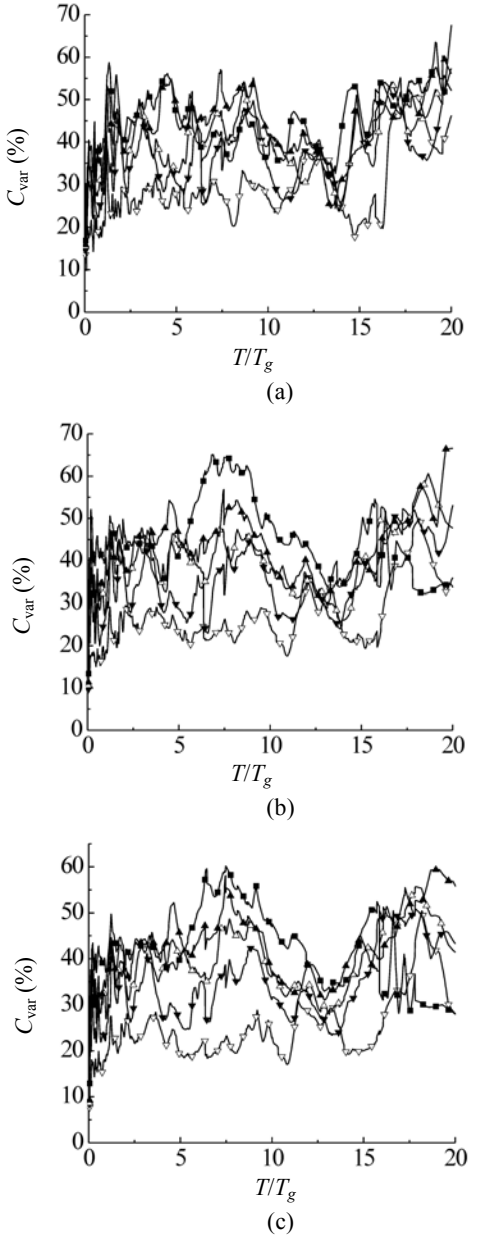

Fig.13 Covariance of SFMC in Site type II for shear-slipped model. (a) Damping ratio 0.02; (b) Damping ratio 0.0235; (c) Damping ratio 0.05

The standardized SFMC spectra for a given ductility, given damping and post-yield stiffness, was calculated using all earthquake records belonging to the same site condition. They were put together to carry out a statistical regression analysis. The averaged spectra were found. Covariance spectrum is also given for each set of parameters.

It was found that the most important factor determining R is the ductility. R approximatively increases linearly with ductility. The energy-dissipating capacity, damping and the post-yield stiffness are the less important factors influencing R. The equal energy criterion is not applicable in the short period range according to statistical results.

R increases with energy dissipating capacity in the short period range, but its effect is reduced in the moderate period range. In the long period range the effect of energy-dissipating capacity is not obvious. So it may be concluded that the energy dissipating capacity is important only for structures with short period and moderate period ($0.3 \leq T/T_g < 5.0$).

For EPP and ELH models, R decreases with increasing damping; R for 0.05 damping is 10% to 15% smaller than that of R for 0.02 damping. For the shear slip model and the bilinear elastic model, the difference in the effects of the damping is not obvious.

For EPP and ELH models, greater post-yield stiffness leads to greater R, but the influence of post-yield stiffness is obvious only when the post yield stiffness is less than 10% of the initial stiffness. Post-yield stiffness has greater influence when the ductility is large.

By means of statistical regression analysis the relation of the seismic force modification factor R with the natural period of the system and ductility for EPP and ELH models was established for each site and soil condition. This will help to improve the seismic design of steel structures.

References

Borzi, B., Elnashai, A.S., 2000. Refined force reduction factors for seismic design. *Engineering Structures*, **22**:1244-1260.

Fajfar, P., 1995. The 10th European Conf. on Earthquake Engineering, Balkema, p.2969-2974.

Huang, J.Q., 2005. Elastic-plastic Dynamics and Aseismic Design Theory of Steel Structures. Ph.D Thesis, Zhejiang University, p.103-147 (in Chinese).

Kappos, A.J., 1999. Evaluation of behavior factors on the basis of ductility and overstrength studies. *Engineering Structures*, **21**:823-835.

Krawinkler, H., Nassar, A.A., 1992. Seismic Design Based on Ductility and Cumulative Damage Demand and Capacities. *In*: Fajfar, K.(Ed.), Nonlinear Seismic Analysis and Design of Reinforced Concrete Buildings. Elsevier Applied Science, New York.

Li, H.L., Sang, W.H., Young, H.O., 1999. Determination of ductility factor considering different hysteretic models. *Earthquake Engineering and Structural Dynamics*, **28**:957-977.

Miranda, E., 1993. Site-dependent strength-reduction factors. *Journal of Structural Engineering*, **119**:3503-3519.

Miranda, E., Bertero, V.V., 1994. Evaluation of strength reduction factor for earthquake-resistance design. *Earthquake Spectra*, **10**(3):357-379.

Newmark, N.M., Hall, W.J., 1982. Earthquake Spectra and Design. EERI Monograph Series, Oakland.

Vidic, T., Fajfar, P., Fischinger, M., 1994. Consistent inelastic design spectra: strength and displacement. *Earthquake Engineering and Structural Dynamics*, **23**:507-521.

Xu, Z.X., Yu, A.D., 1998. Discuss about seismic influence coefficient. *Engineering Mechanics Supplement*, p.100-107 (in Chinese).

Zhuo, W.D., Fan, L.C., 2001. On strength reduction factors used for seismic design of structures. *Earthquake Engineering and Engineering Vibration*, **21**(1):84-88 (in Chinese).